

Thermoresponsive Self-Assembled Nanovesicles Based on Amphiphilic Triblock Copolymers and Their Potential Applications as Smart Drug Release Carriers

Xia Cao,¹ Yunxiang Chen,¹ Wenchao Chai,¹ Wenjie Zhang,¹ Yudong Wang,¹ Peng-Fei Fu²

¹School of Material Science and Engineering, Zhengzhou University, Zhengzhou 450001, China

²Dow Corning Corporation, Midland, Michigan 48686

Correspondence to: Y. Wang (E-mail: wyd@zzu.edu.cn) and P.-F. Fu (E-mail: pengfei.fu@dowcorning.com)

ABSTRACT: A series of thermoresponsive triblock copolymers, methoxy poly(ethylene oxide)-*b*-poly(ϵ -caprolactone)-*b*-poly(*N*-isopropylacrylamide) (mPEO-*b*-PCL-*b*-PNIPAM), with different PCL and PNIPAM block lengths, were synthesized by a combination of ring opening polymerization and reversible addition-fragmentation chain transfer polymerization techniques. The triblock copolymers undergo self-assembly in aqueous solutions forming stable nanovesicles of various sizes with a lipid membrane structure similar to body cells as revealed by transmission electron microscopy. The nanovesicle is thermoresponsive, that is, its size is tunable using the temperature as a switch: shrinks at a temperature above the lower critical solution temperature (LCST) and expands at a temperature below the LCST. The corresponding LCST of the triblock copolymers is adjustable by varying the PNIPAM segment length as well as the PCL segment length and covers a range from 33.9 to 41.0°C in water. The diameter of nanovesicles for mPEO_{5k}-*b*-PCL_{5k}-*b*-PNIPAM_{13.2k} is about 177.7 nm below the LCST and 138.9 nm above the LCST, as determined by dynamic light scattering. It was demonstrated using indomethacin, a popular anti-inflammation medicine, that the triblock copolymers can effectively act as a drug release carrier under the right human physiological conditions, that is, store the drug at a lower temperature and release it at a higher temperature, possibly targeting at the lesion sites of human body. © 2014 Wiley Periodicals, Inc. *J. Appl. Polym. Sci.* **2015**, *132*, 41361.

KEYWORDS: biomaterials; copolymers; drug delivery systems; self-assembly; stimuli-sensitive polymers

Received 14 June 2014; accepted 1 August 2014

DOI: 10.1002/app.41361

INTRODUCTION

The search for a well controlled self-assembled polymer nanovesicle system as a drug release carrier in medical sciences is of great interest recently,^{1–9} for it offers many potential benefits in comparison to the conventional system, such as increasing the solubility of hydrophobic drugs in water, prolonging the drug's circulation time, improving the target distribution, and having a better controlled release rate.¹⁰ However, the construction of such a well balanced polymer system has been a great challenge that requires meticulous design and precise synthesis of targeted block copolymers with right properties and lengths, capable of forming self-assembled nanovesicles in aqueous solutions under the right physiological conditions.

Different aggregate morphologies can be produced from block copolymer solutions,¹¹ including spheres, rods, lamellae, vesicles, and other related structures. Typically morphology can be controlled by varying copolymer composition, initial copolymer concentration, the type of solvents, the amount of water present in solvent mixtures, the solution temperature, and the

selection of additives. Among the various morphologies, vesicle morphology has received special attention because of its resemblance to the cellular structure which is ideal for drug delivery applications.¹² In particular, amphiphilic polymers are of great interests, for the polymers not only possess the properties of a typical drug carrier, but also offer many other unique properties.^{4,13,14} These properties include great biocompatibility due to the liposome structure, great mechanical property due to the membrane nature, which enhances the liposome stability and lowers the osmosis. In addition, the polymers normally have both a large hydrophilic inner-chamber and a large hydrophobic exterior membrane, capable of simultaneously encapsulating and carrying hydrophilic drugs as well as hydrophobic drugs.

Most of previous work has been focused on using poly(ethylene oxide)-poly(ϵ -caprolactone) (PEO-PCL) diblock copolymers as drug delivery carriers.^{15,16} As a hydrophilic component with good biocompatibility, the PEO block acts as a stabilizer for the diblock copolymers in aqueous solutions; and it has been approved by United States Food and Drug Administration (FDA) for use in medical treatment since it lacks

immunogenicity and is easy to be recycled from the human body.^{17,18} Likewise PCL is a hydrophobic polyester unit with good biocompatibility and degradability, and has also been approved by FDA for medical applications.^{19,20} It is known that lesion sites of human body in most cases show different characteristics from the normal parts of human body, such as temperatures and pH values. As a result one can target the drug releases selectively at lesion sites according to the physiological or chemical responses from different stimulus.^{21,22} However, these diblock copolymers are not as selective or “intelligent” as desired due to the lack of environmental responsive properties.

Thermosensitive polymers that use the temperature as a stimulus are not only effective but also easy to apply. Among thermoresponsive polymers, poly(*N*-isopropylacrylamide) (PNIPAM), has been widely studied, since its lower critical solution temperature (LCST) in water is around 32°C,²³ close to the human body temperature (37°C). Upon heating the polymer undergoes a phase transition in an aqueous solution from hydrophilic (below the LCST) to hydrophobic (above the LCST). In addition the transition can also be affected by varying the hydrophilic monomer–hydrophobic monomer ratio. Consequently the incorporation of a thermoresponsive block, such as PNIPAM, into the PEO-PCL block copolymers is expected to greatly improve their properties as a drug delivery candidate in aqueous solution. Interestingly the copolymers made up of these three individual blocks (ABC) have received little attention, whereas majority of the previous research is centered on AB and ABA block copolymers, such as PEO-PCL,¹⁵ PEO-PNIPAM,^{24–28} PCL-PNIPAM,²⁹ PNIPAM-PEO-PNIPAM,^{28,30} and PCL-PNIPAM-PCL.³

Typically AB or ABA types of amphiphilic block copolymers are more likely to self-assemble into vesicles with a symmetrical bimolecular membrane structure.³¹ Recently both Meier's group^{32,33} and Eisenberg's group^{34,35} proposed that some of the ABC triblock polymers that may also be capable of self-assembling into asymmetrical vesicles as long as the ABC triblock copolymers satisfy the following requirements: (1) A and C are two different water soluble blocks; (2) the middle block B is a hydrophobic block. In this context, we have designed and synthesized a series of mPEO-*b*-PCL-*b*-PNIPAM triblock copolymers with different PCL and PNIPAM block lengths using a ring-opening polymerization (ROP) method and a reversible addition-fragmentation chain transfer (RAFT) polymerization method. The selection of these blocks was based on their relative hydrophilicity, biocompatibility, thermoresponsive property, and low toxicity. It is expected that the triblock copolymer would self-assemble into an asymmetrical vesicles in aqueous solutions, which can controllably release drugs using the temperature “switch.” For this study, indomethacin (IMC), a popular hydrophobic antibiotic, was selected as a model medicine to investigate the release properties of the system. It is found that the current triblock copolymer can effectively act as a drug release carrier, that is, store the drug at a lower temperature and release it at a higher temperature, possibly targeting at the lesion sites of human body.

EXPERIMENTAL

Materials

Ethylene oxide (EO) (Shanghai Jingfeng Chemical Reagent) was dried with CaH₂ for 48 h and then distilled under N₂ and

stored at –22°C prior to use. ϵ -Caprolactone (CL, 99%, Acros Organics) was dried over calcium hydride (CaH₂) and distilled under reduced pressure before use. NIPAM (97%, Aldrich) and 2, 2-azobisisobutyronitrile (AIBN, 98%, Aldrich) were purified by recrystallization twice from *n*-hexane and ethanol. Toluene and 1,4-dioxane were dried over CaH₂ and distilled before use. Tetrahydrofuran (THF) was refluxed in the presence of metallic potassium under nitrogen and distilled before used. 3-Benzylsulfanylthiocarbonyl-sufanylpropionic acid (BSPA) was synthesized according to the literature.³⁶ 1, 3-Dicyclohexylcarbodiimide (DCC, 99%, Alfa Aesar) and 4-(*N*, *N*-dimethylamino)pyridine (DMAP, 99%, Alfa Aesar) and all other reagents were used as received.

Representative Syntheses of Amphiphilic Block Copolymers mPEO-*b*-PCL

Prewighted amount of mPEO ($M_n = 2950$, 3.80 g) was added to a round bottom flask and dissolved by toluene (50 mL) in order to remove the water by azeotropic distillation. Then 15 mL dried toluene, preweighted amount of CL (6.2 g, 5.8 mL) and Sn(Oct)₂ (0.25 g, 0.2 mL) were added. The mixture was transferred from flask to an ampoule, which was degassed by triple freeze-pump-thaw cycles at the temperature of liquid nitrogen. Furthermore, the polymerization was carried out at 100°C for 24 h with vigorous stirring. Finally the reaction product was collected by filtration and purified three times by dissolution/precipitation with methylene chloride/ diethyl ether, and then dried under vacuum at 30°C for 24 h. Copolymers with different EO/CL ratios were prepared under the similar conditions.

Synthesis of Macromolecule-RAFT Agent (PEO-*b*-PCL-BSPA)

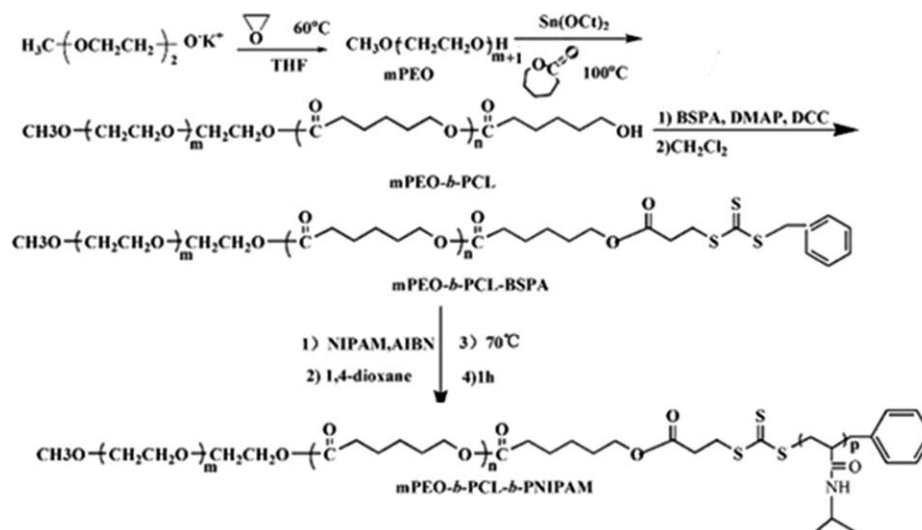
Typically mPEO-*b*-PCL(8.9 g, 1.1 mmol, $M_n = 8000$) was dissolved in anhydrous dichloromethane; then BSPA (0.4539 g, 1.65 mmol) and DMAP (0.14 g, 1.1 mmol) were added. After the mixture was stirred at 0°C for 0.5 h, DCC (0.34 g, 1.65 mmol) was added. Next, the reaction mixture was allowed to polymerize while stirring at room temperature for 12 h; an insoluble precipitate, 1,3-dicyclohexylurea, was formed during the reaction process and was removed by filtration. The remaining solution was purified by dissolving in dichloromethane and precipitating with diethyl ether until unreacted BSPA was removed completely to yield the title triblock copolymer, PEO-*b*-PCL-BSPA.

Synthesis of PEO-*b*-PCL-*b*-PNIPAM Triblock Copolymers

The triblock copolymers were synthesized through RAFT polymerization. Typically, NIPAM (2.0 g), mPEO-*b*-PCL-BSPA (1.0 g), and AIBN (4.9 mg) were dissolved in 1,4-dioxane (20 mL) and degassed under reduced pressure by triple freeze-pump-thaw cycles. Then, the polymerization was carried out at 70°C for 1 h with vigorous stirring. The product was collected by filtration and purified three times by dissolution/precipitation with methylene chloride/ diethyl ether, and dried in vacuum overnight. The detailed reaction conditions using the RAFT polymerization to synthesize mPEO-*b*-PCL-*b*-PNIPAM copolymers are listed in Table II.

NMR and Gel Permeation Chromatography Characterizations

The chemical structures of the products from each synthetic step were characterized by ¹H NMR (DMX 400 MHz



Scheme 1. Synthetic scheme for making triblock mPEO-*b*-PCL-*b*-PNIPAM copolymers.

spectrometer with tetramethylsilane as the internal standard) using CDCl₃ or D₂O as solvents. The molecular weight and its distribution (M_w/M_n) of the polymers were determined by gel permeation chromatography (GPC). GPC was performed on an Agilent1100 with a G1310A pump, a G1362A refractive detector, and a G1314A variable wavelength detector, and THF was used as eluent at 35°C at 1.0 mL/min. One 5 μ m LP gel column (500 Å, molecular range $500^{-2} \times 10^4$ g/mol) and two 5 μ m LP gel mixed bed column (molecular range $200^{-3} \times 10^6$ g/mol) were calibrated with polystyrene standard samples.

The Measurement of Critical Aggregation Concentration for mPEO-*b*-PCL-*b*-PNIPAM by Fluorescence Spectrophotometer

The critical aggregation concentration (CAC) measurement was assisted with the addition of pyrene. First of all, a weighted amount of pyrene was dissolved in acetone and diluted with DI-water to a solution with a concentration of 6.4×10^{-7} mol/L; in a separate flask, a weighted amount of mPEO-*b*-PCL-*b*-PNIPAM was dissolved in THF to make a solution with a concentration of 0.01 mg/mL, 0.05 mg/mL, 0.1 mg/mL, 0.5 mg/mL, and 1 mg/mL in THF, respectively. Next, take a weighted amount of the triblock copolymer THF solution, and then mix with 5 mL of the above pyrene solution to make a series of

polymer samples with concentration from 10^{-4} g/mL to 10^{-9} g/mL. After removing the organic solvent, the solution was measured using a Hitachi F-4600 Fluorescence spectrophotometer at 25°C with an excited light wavelength of 339 nm. The fluorescence intensity was recorded at two emission wavelengths (382 nm and 372 nm), and the CAC of the copolymer was derived from the plot of I_{372}/I_{382} versus concentration.

Self-Assembly of mPEO-*b*-PCL-*b*-PNIPAM

mPEO-*b*-PCL-*b*-PNIPAM triblock copolymer nanovesicles were prepared according to the dialysis method. Firstly mPEO-*b*-PCL-*b*-PNIPAM copolymer (5.0 mg) was dissolved in 1 mL of THF followed by the addition of 5 mL of distilled water to the stirring solution. The mixture was stirred for 4 h and the solution was then dialyzed against 1000 mL of distilled water for 24 h using a dialysis tube (molecular weight cut off: 8000–12,000 g/mol), during which the distilled water was replaced every 8 h.

Thermosensitivity of mPEO-*b*-PCL-*b*-PNIPAM Nanovesicles

The LCST of mPEO-*b*-PCL-*b*-PNIPAM was determined by a cloud point method. The optical transmittance of the copolymer aqueous solution (1 mg/mL) at various temperatures was

Table I. Summary and Characterization of mPEO, mPEO-*b*-PCL, and mPEO-*b*-PCL-*b*-PNIPAM Polymers

Sample	M_n^a ($\times 10^3$)	M_n^b ($\times 10^3$)	M_w/M_n^c	Block length (M_n)		
				PEO	PCL	PNIPAM
mPEO _{3k}	3.8	2.95	1.07	3,000	0	0
mPEO _{3k} - <i>b</i> -PCL _{5.0k}	11.53	7.90	1.33	3,000	5,000	0
mPEO _{3k} - <i>b</i> -PCL _{7.5k}	14.30	10.50	1.36	3,000	7,500	0
mPEO _{3k} - <i>b</i> -PCL _{5k} - <i>b</i> -PNIPAM _{4.0k}	15.84	11.80	1.42	3,000	5,000	4,000
mPEO _{3k} - <i>b</i> -PCL _{5k} - <i>b</i> -PNIPAM _{13.2k}	23.09	21.20	1.43	3,000	5,000	13,200
mPEO _{3k} - <i>b</i> -PCL _{5k} - <i>b</i> -PNIPAM _{16.5k}	28.72	25.00	1.48	3,000	5,000	16,500

^a By GPC (vs. PS).

^b By the ¹H NMR data.

^c By GPC (vs. PS).

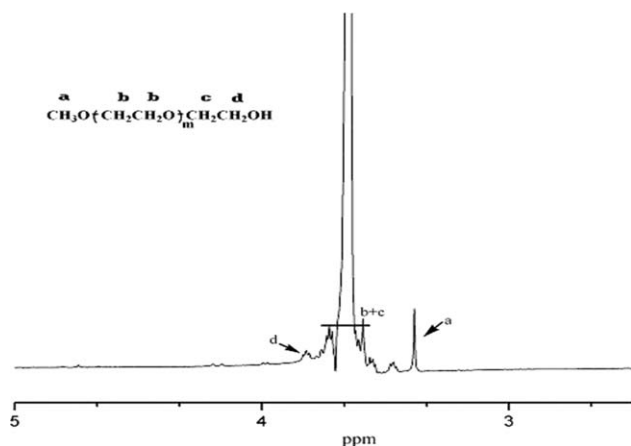


Figure 1. The ^1H NMR spectrum of mPEO in CDCl_3 .

measured at 500 nm by UV-vis spectroscopy (Agilent). The temperature was carried out at 2°C intervals, from 25 to 49°C , and the sample were kept at each temperature for 15 min. The LCST of the copolymers was defined as the temperature with a half of the optical transmittance between below and above transitions.

Size Distribution Measurement by Dynamic Light Scattering

The size and size distribution of mPEO-*b*-PCL-*b*-PNIPAM nanovesicles were measured by dynamic light scattering (DLS), using a Malvern Instrument Zetasizer Nano ZS using 633 nm red laser at 173° scattering angle at various temperatures. An aqueous solution of mPEO-*b*-PCL-*b*-PNIPAM nanovesicles with various compositions was added into a sample cell thermostated at a given temperature between 25 and 45°C for 3 min prior to the measurement. To investigate the stability of nanovesicles in aqueous solution at temperatures above and below the LCST, the sample cell was thermostated at 25°C for 15 min and 40°C for 15 min, and the nanovesicle size was measured at each individual temperature.

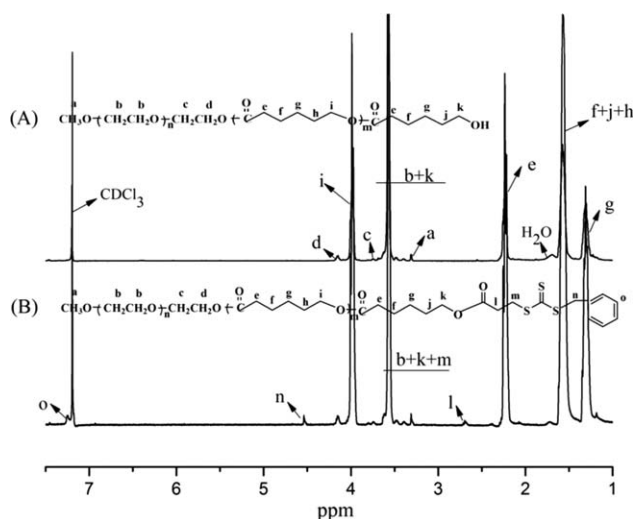


Figure 2. The ^1H NMR spectra of mPEO-*b*-PCL (A) and mPEO-*b*-PCL-BSPA (B) in CDCl_3 .

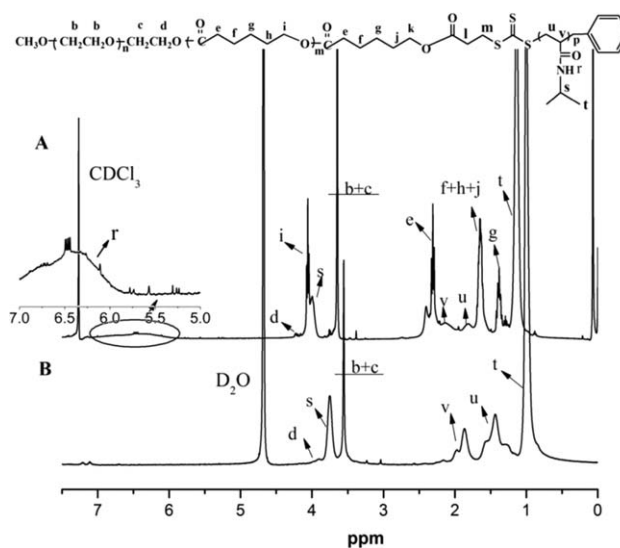


Figure 3. The ^1H NMR spectra of mPEO-*b*-PCL-*b*-PNIPAM in CDCl_3 (A) and D_2O (B).

Transmission Electron Microscopy Measurements

Transmission electron microscopy (TEM) measurements were done with the aid of an electron microscope (FEI TECNAI G2 20) at an acceleration voltage of 200 kV. The TEM samples were prepared in a water bath at a constant temperature: a drop of the nanovesicle solution, which was pre-thermostated at either 25°C or 45°C , was deposited onto a preheated copper grid, and dried at the same temperature under atmospheric pressure.

Drug Loading and *In Vitro* Drug Release

The triblock copolymer (10 mg) and IMC (2.5 mg) were dissolved in 5 mL THF. The solution was placed into a dialysis tube (molecular weight cut off: 7000 g/mol) and dialyzed against 2 L distilled water for 24 h, and the distilled water was replaced every 8 h in order to remove the unloaded free drug and THF. Subsequently the dialysis tube was directly immersed into 50 mL PBS (pH 7.4). A volume of 3 mL was withdrawn from the PBS periodically. The volume of solution was held constant by adding 3 mL PBS after each sampling. The concentration of the released IMC was measured with a UV spectrophotometer (Shimadzu UV-3010) at 320 nm. To determine the entrapment efficiency (EE), the drug-loaded nanovesicles solution was lyophilized, and disrupted in DMF and analyzed by UV absorbance. The EE and drug loading (DL) are defined by the following equations:

$$\text{EE} = \left(\frac{\text{mass of drug loaded in micelles}}{\text{mass of drug fed initially}} \right) \times 100\%$$

$$\text{DL} = \left(\frac{\text{mass of drug loaded in micelles}}{\text{mass of drug-loaded micelles}} \right) \times 100\%$$

RESULTS AND DISCUSSION

Synthesis and Characterization of mPEO-*b*-PCL-*b*-PNIPAM

A new pathway consisting of four steps to synthesize the mPEO-*b*-PCL-*b*-PNIPAM triblock copolymers is shown in Scheme 1. First the linear mPEO was prepared by anionic ring-opening copolymerization of cyclic EO using 2-(2-methoxyethoxy) ethoxide potassium as an initiator. It was subsequently

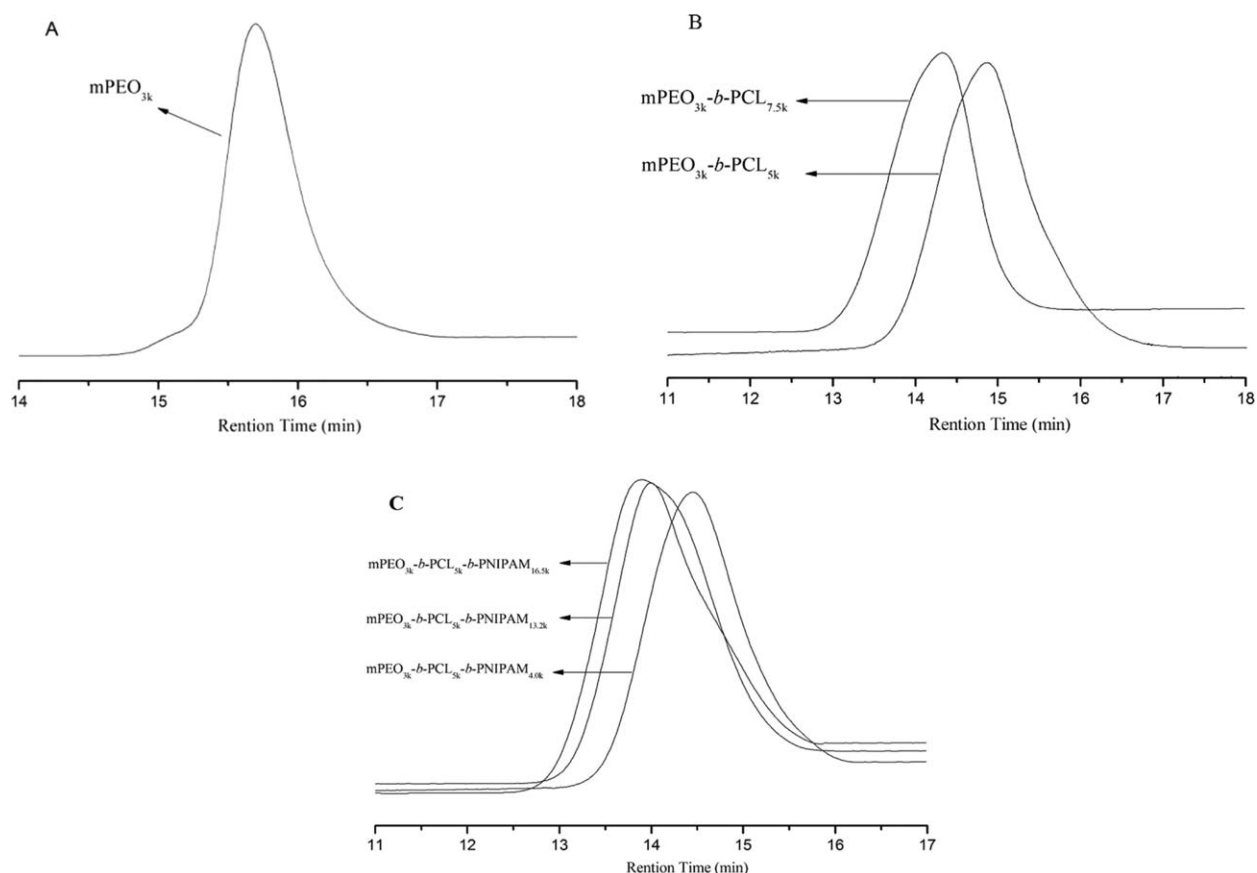


Figure 4. GPC traces of mPEO (A), mPEO-*b*-PCL (B), and mPEO-*b*-PCL-*b*-PNIPAM (C).

brought to react with CL to form mPEO-*b*-PCL diblock copolymers via a ROP mechanism in the presence of Sn(Oct)₂ as a catalyst. Then the hydroxyl capped diblock copolymer was allowed to react with BSPA to form mPEO-*b*-PCL-*b*-BSPA. In the last step a RAFT polymerization of NIPAM was performed in 1,4-dioxane at 70°C with AIBN as an initiator and the mPEO-*b*-PCL-*b*-BSPA as the macromolecular chain transfer agent. The polymer obtained from each individual step was isolated and characterized (Table I, vide infra).

Since a well controlled PEO unit needs to be constructed as the first block, the ROP of cyclic EO, with 2-(2-methoxyethoxy)

ethoxide potassium as the initiator, was conducted at 60°C in THF; whereby a monodispersed PEO polymer with a degree of polymerization (DP) around 80 was obtained (GPC: $M_n = 3.80 \times 10^3$, $M_w/M_n = 1.07$). The ¹H-NMR of the mPEO is shown in Figure 1. The signal at around 3.38 ppm is from the methyl protons of mPEO, and the signal from 3.6 to 3.7 ppm is attributed to the methylene protons of (CH₂CH₂O) repeating units. The number molecular weight (M_n) of mPEO can be also obtained from the end group analysis according to the eq. (1), wherein A_a is the integration of terminal methyl protons and A_b is the integration of the methylene protons.

Table II. Influence of the Reaction Time on the RAFT Polymerization of NIPAM in 1,4-dioxane at 70°C Using mPEO_{3k}-*b*-PCL_{7.5k} as the RAFT Agent

Sample	Time (min)	PNIPAM ^a (DP)	Conversion (%)	Block length (M_n) ^a			M_w/M_n ^b
				PEO	PCL	PNIPAM	
A	90	11	7.43	3,000	7,500	1,261	1.3
B	110	36	24.2	3,000	7,500	4,099	1.32
C	120	56	37.4	3,000	7,500	6,348	1.35
D	150	93	62.5	3,000	7,500	10,610	1.29
E	180	144	95.9	3,000	7,500	16,270	1.34

^a Number-average molecular weight (M_n) calculated from the ¹H NMR data.

^b Molecular weight distribution (M_w/M_n) determined by GPC, calibrated against PS standards.

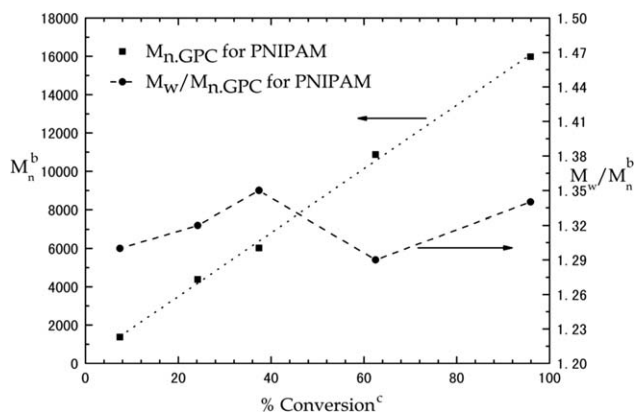


Figure 5. The plot of polymer molecular weight and polydispersity on % monomer conversion in 1,4-dioxane at 70°C using mPEO-*b*-PCL-*b*-BSPA as RAFT agent for an initial ratio [RAFT agent] / AIBN = 4, [NIPAM] / [the RAFT agent] = 150 (^bdetermined by GPC, calibrated against PS standards; ^cmonomer conversion as determined by ¹H NMR spectroscopy).

$$M_{n(\text{mPEO})} = \frac{A_b/4}{A_a/3} \times 44.05 \quad (1)$$

For the mPEO-*b*-PCL diblock copolymer synthesized in the second step, five extra signals at 4.19, 3.99, 2.25, 1.59, and 1.31 ppm, characteristic of PCL repeat units, were observed in its ¹H-NMR spectrum [Figure 2(A)]. The chain length of PCL can be controlled by varying molar ratio of CL monomer to mPEO. For the mPEO-*b*-PCL-BSPA copolymer, a new group of signals (2.69, 3.55, 4.55, and 7.26 ppm) appeared in its ¹H-NMR spectrum, characteristic of BSPA [Figure 2(B)]. The corresponding molecular weight of the copolymers can be also obtained via the end-group analysis according to the eq. (2), wherein A_a is the integration of terminal methyl protons and A_g is the integration of the methylene protons as shown in Figure 2.

$$M_{n(\text{mPEO-}b\text{-PCL})} = \frac{A_g/2}{A_a/3} \times 114 + M_{n(\text{mPEO})} \quad (2)$$

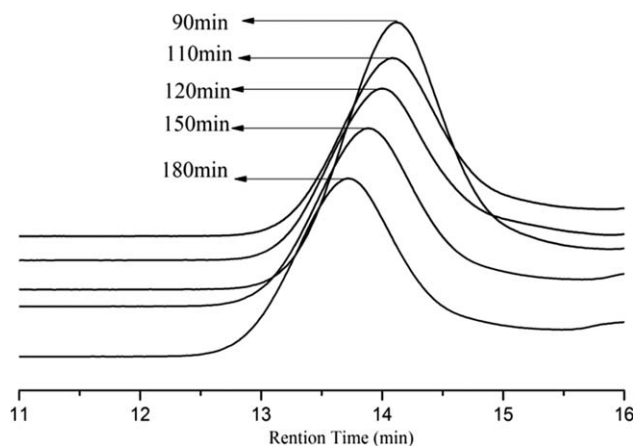


Figure 6. GPC traces of the triblock copolymers mPEO_{3k}-*b*-PCL_{7.5k}-*b*-PNIPAM_{16.2k} formed at different reaction times. [RAFT agent] / AIBN = 4, [NIPAM] / [the RAFT agent] = 150.

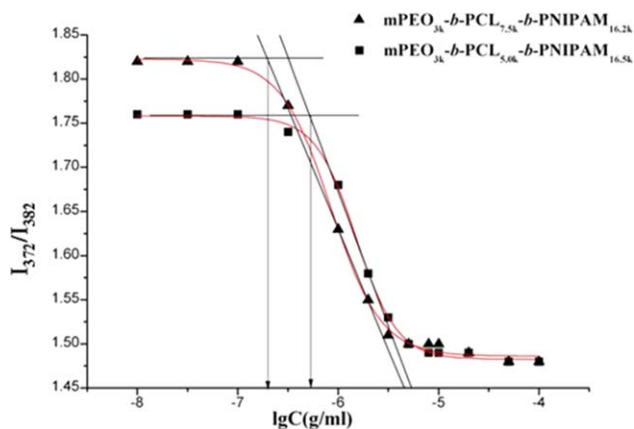


Figure 7. The plot of I_{372}/I_{382} as a function of the triblock copolymer concentration in an aqueous solution in the presence of pyrene as the fluorescent probe. [Color figure can be viewed in the online issue, which is available at wileyonlinelibrary.com.]

For the mPEO-*b*-PCL-*b*-PNIPAM triblock copolymer made in the final step, new signals due to the PNIPAM block at 3.93 ppm from -CH(CH₃)₂, 2.05 ppm from -CH₂CH-, 1.76 ppm from -CH₂CH-, and 1.06 ppm from -CH(CH₃)₂ were observed in CDCl₃, in addition to the signals from the mPEO and PCL blocks [Figure 3(A)]. When the polymer was dissolved in D₂O, only signals due to the hydrophilic PNIPAM and mPEO units were observed in its ¹H NMR spectrum [Figure 3(B)] as expected.

The molecular weight of copolymers can also be calculated via the end group analysis according to the eq. (3), wherein A_u is the integration of protons at the *u*-carbon. Figure 4 shows the GPC traces of mPEO (A), mPEO-*b*-PCL diblock copolymer (B), and mPEO-*b*-PCL-*b*-PNIPAM (C), and their corresponding molecular weight data is summarized in Table I. The triblock copolymer with the longest PNIPAM chain has a structure of mPEO_{3k}-*b*-PCL_{5k}-*b*-PNIPAM_{16.5k} and a low polydispersity (PDI < 1.5) even after a four-step synthesis. Remarkably even at such a very high molecular weights (M_n), the triblock copolymer remains unimodal.

$$M_{n(\text{mPEO-}b\text{-PCL-}b\text{-PNIPAM})} = \frac{A_u/2}{A_a/3} \times 113 + M_{n(\text{mPEO})} + M_{n(\text{PCL})} \quad (3)$$

For the last step (RAFT polymerization) of the triblock copolymer synthesis, the polymerization process was monitored by periodically taking out an aliquot of polymer sample and analyzing it using GPC and NMR techniques (Table II). It was observed that after an introduction period of 90 min, whereby the RAFT equilibrium was established, the copolymer molecular weight increases gradually with the reaction time until all of the NIPAA monomer is consumed in 1,4-dioxane with a RAFT agent/AIBN ratio of 4.0 mol/mol and a NIPAM/the RAFT agent ratio of 150. A plot of the polymer molecular weight with the monomer conversion shows almost a linear relationship, indicating a living polymerization nature (Figure 5).³⁷ It is worthy of note that the polydispersity of the diblock copolymer mPEO_{3k}-*b*-PCL_{7.5k} is a little higher than desired as a RAFT

Table III. The Block Length and CAC of the Triblock Copolymers

Sample	Block length (M_n)			CAC ($\times 10^{-7}$) g/mL	M_w/M_n^a
	PEO	PCL	PNIPAM		
mPEO _{3k} -b-PCL _{5.0k} -b-PNIPAM _{16.5k}	3,000	5,000	16,500	5.128	1.48
mPEO _{3k} -b-PCL _{7.5k} -b-PNIPAM _{16.2k}	3,000	7,500	16,270	1.995	1.34

^a Molecular weight distribution (M_w/M_n) determined by GPC, calibrated against PS standards.

agent due to a number of possible side reactions.³⁸ Nonetheless, the polydispersity of the triblock copolymers subsequently built upon the diblock copolymer remains within a narrow range during the polymerization process, as expected for a RAFT polymerization process. Figure 6 shows the GPC traces of the triblock copolymer, mPEO-*b*-PCL-*b*-PNIPAM, formed at different reaction times in addition to the GPC traces of the corresponding mPEO (3K) polymer and the PEO-PCL diblock copolymers. These results further confirm that the current RAFT polymerization is a well controlled process.

Formation and Properties of Self-Assembled Triblock Copolymer Vesicles

The CAC of a block copolymer is an important parameter assessing its capability of forming polymer vesicles under certain experimental conditions. When the concentration of a block copolymer is below CAC, the copolymer is well dispersed in the solvent media without the formation of any polymer aggregation; when the concentration is above CAC, the copolymer tends to self-assemble together and form vesicles. As a result, the lower the CAC, the higher tendency is for the formation of polymer aggregations or vesicles. It is known that when the polymer vesicle enters a human body as a drug carrier, its concentration will be greatly diluted; as a result a copolymer system

with a lower CAC is required for drug release applications since it will allow a longer circulation time and avoid any premature release of the intended drugs in the body.

For the current study pyrene was used as the fluorescent probe to measure the CAC of the block copolymers. With the increase of the block copolymer's concentration, the fluorescent intensity raises accompanied with the maximal peak shift from 372 to 382 nm, although the amount of pyrene remains constant in the solution. The maximal peak shift was due to the formation of self-assembled nanovesicles which allows more pyrene to enter the hydrophobic core of the copolymer vesicles. The CAC of the copolymers can be calculated from the plot of I_{372}/I_{382} versus concentration (Figure 7). Based on the current method, the CAC of triblock copolymers with different PCL lengths was determined. As summarized in Table III, the CAC for both of the triblock copolymers is in the order of 10^{-7} g/mL. This means that the copolymers can form nanovesicles even at an extremely low concentration. In addition it was found that increasing the PCL block length lowers the corresponding CAC of the copolymers, suggesting that the copolymers have a higher tendency to form aggregates under the circumstances.

As mentioned before, PNIPAM is a well established thermoresponsive polymer with a LCST around 32°C in water. It is

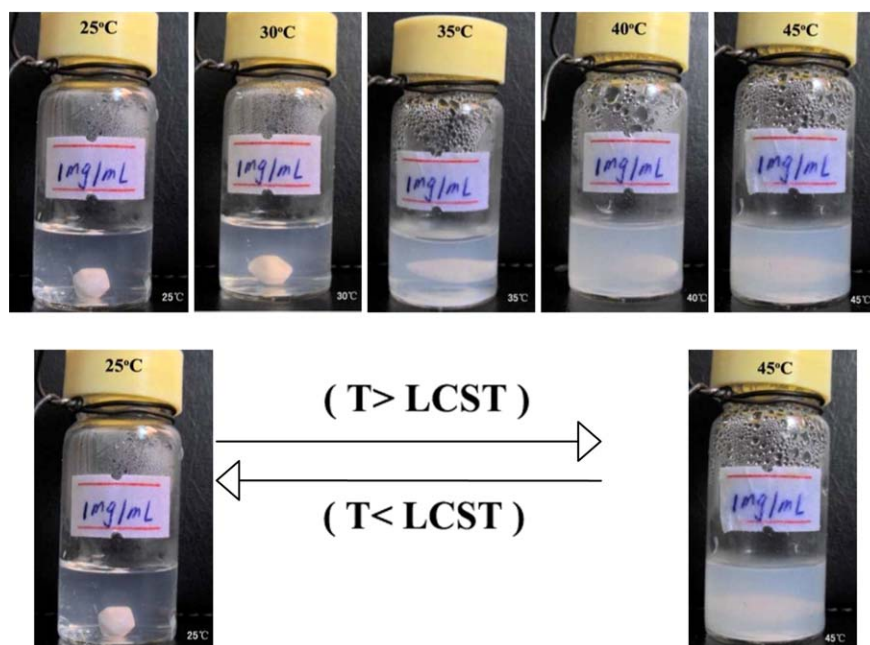


Figure 8. Visual appearance of the aqueous solution of mPEO_{3k}-*b*-PCL_{5k}-*b*-PNIPAM_{16.5k} at temperatures below and above LCST.

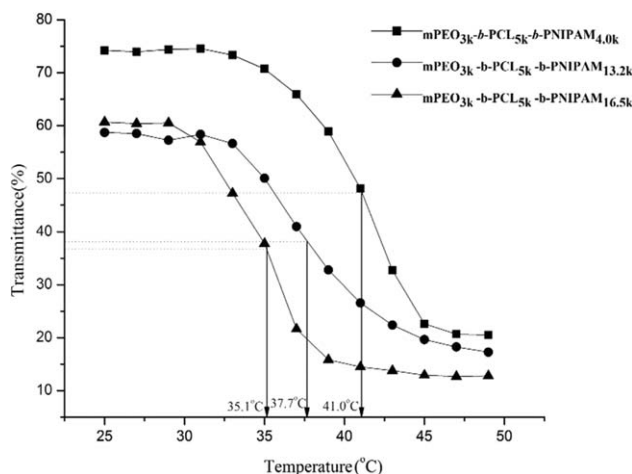


Figure 9. Optical transmittance of aqueous solutions of mPEO-*b*-PCL-*b*-PNIPAM triblock copolymers at different temperatures with the fixed PEO and PCL blocks but different length of PNIPAM (concentration: 1 mg/mL). The measurement wavelength is 500 nm.

molecularly soluble in water below its LCST but becomes insoluble above this temperature. Thus, it is interesting to investigate the phase as well as morphological changes of an amphiphilic block copolymer containing a PNIPAM block in aqueous solutions simply by varying the solution temperature.

As revealed in Figure 8, triblock copolymer mPEO_{3k}-*b*-PCL_{5k}-*b*-PNIPAM_{16.5k} exhibits a phase transition when the temperature was raised from 25 to 45°C: the copolymer solution changes from translucent to turbid gradually. Remarkably this phase transition is reversible and occurs within a narrow temperature range. This observation was consistent with the optical transmittance measurements of the copolymer solutions in water, which shows the optical transmittance of triblock copolymer mPEO-*b*-PCL-*b*-PNIPAM solutions at 500 nm wavelength, with fixed PEO and PCL block lengths but different PNIPAM block length, as a function of solution temperature (Figures 9 and 10,

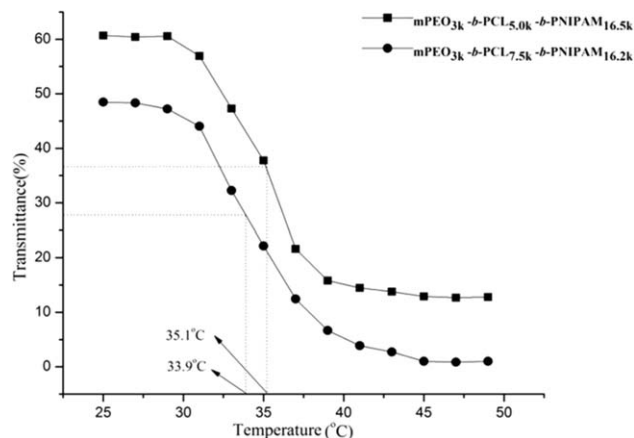


Figure 10. The change of optical transmittance of mPEO-*b*-PCL-*b*-PNIPAM triblock copolymer solution (concentration = 1 mg/mL) at different temperatures with fixed PEO and PNIPAM blocks but different PCL block). The measurement wavelength is 500 nm.

vide infra). When the solution temperature was increased to a temperature above 30°C, the optical transmittance drops abruptly and displays an inverse “S” behavior. This is because at a lower temperature (below LCST) the PNIPAM block of the triblock copolymers acts as a hydrophilic component, and is fully extended and solvated in the aqueous solution via the hydrogen bonding of the amide group of PNIPAM with water; when the temperature is increased to above LCST, the hydrogen bond breaks and the polymer becomes hydrophobic and insoluble due to the presence of isopropyl groups in the PNIPAM blocks in the aqueous solution.

The LCST of the copolymers was determined as a temperature where the optical transmittance is at 50% between the value below and above transitions. It was found that the LCST of the mPEO-*b*-PCL-*b*-PNIPAM, with fixed PEO and PCL block lengths, is 41.0°C, 37.7°C, and 35.1°C when the block length (M_n) of PNIPAM is 4000, 13,200, and 16,500, respectively. This phenomenon can be understood in terms of the chain length

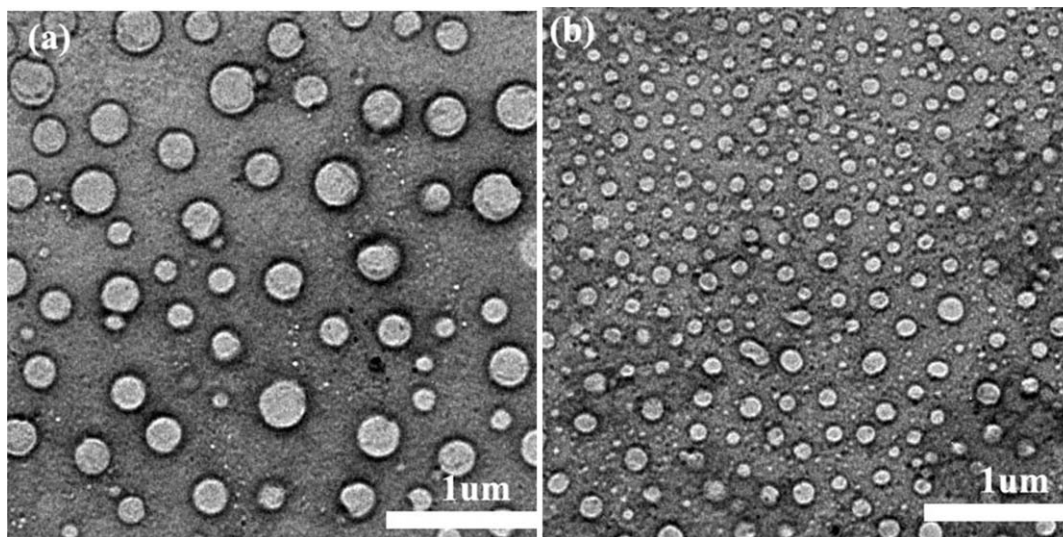


Figure 11. TEM images of mPEO_{3k}-*b*-PCL_{5k}-*b*-PNIPAM_{16.5k} nanovesicles at 25°C (A) and 45°C (B) in distilled water.

Table IV. Characterization of mPEO-*b*-PCL-*b*-PNIPAM Nanovesicles with Fixed Length of PEO and PCL Blocks but Different Lengths of PNIPAM Block

Sample	PNIPAM block (M_n)	LCST ($^{\circ}\text{C}$)	Z-average Diameter (nm)		PDI	
			25 $^{\circ}\text{C}$	40 $^{\circ}\text{C}$	25 $^{\circ}\text{C}$	40 $^{\circ}\text{C}$
mPEO _{3k} - <i>b</i> -PCL _{5k} - <i>b</i> -PNIPAM _{4.0k}	4,000	41.0	149.7	132.4	0.308	0.302
mPEO _{3k} - <i>b</i> -PCL _{5k} - <i>b</i> -PNIPAM _{13.2k}	13,200	37.7	177.7	138.9	0.235	0.258
mPEO _{3k} - <i>b</i> -PCL _{5k} - <i>b</i> -PNIPAM _{16.5k}	16,500	35.1	186.6	137.7	0.278	0.282

effect, that is, the LCST of PNIPAM generally decreased with the increase of PNIPAM block size.³⁹ Another possible attribute to the observation is that the interaction between the hydrophilic PEO and PNIPAM segments, which diminishes as the ratio of hydrophilic PEO to PNIPAM decreases. In addition, a longer PCL block of the copolymer also yields a lower LCST values. For example the LCST of mPEO_{3k}-*b*-PCL_{5k}-*b*-PNIPAM_{16.5k} and mPEO_{3k}-*b*-PCL_{7.5k}-*b*-PNIPAM_{16.2k} is 35.1 $^{\circ}\text{C}$ and 33.9 $^{\circ}\text{C}$, respectively, in distilled water (Figure 10). This is possibly due to the fact that a higher percent of the hydrophobic moiety facilitates more chain aggregation. Although the effect of PEO chain length on the LCST of mPEO-*b*-PCL-*b*-PNIPAM triblock copolymers was not investigated here, the work done by Yang and coworkers on mPEO-*b*-PNIPAM diblock copolymers suggests that a longer PEO chain would lead to an increase of the copolymer's LCST, due to the concentration change of the PNIPAM block as well as extra intermolecular hydrogen bonding between PEO and PNIPAM.²⁴

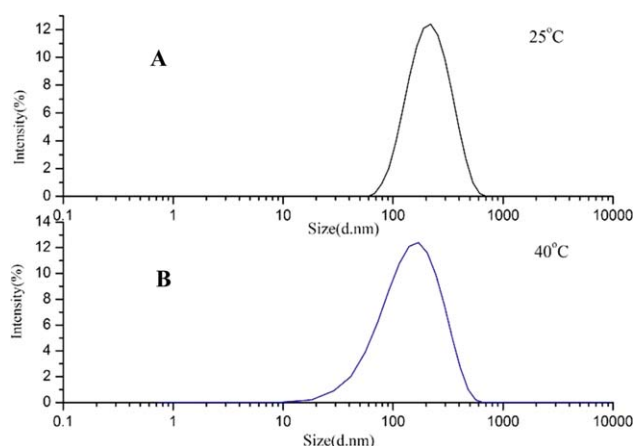
In addition, the morphology of block copolymer mPEO-*b*-PCL-*b*-PNIPAM was investigated using TEM. Figure 11 shows the TEM images of mPEO_{3k}-*b*-PCL_{5k}-*b*-PNIPAM_{16.5k} nanovesicles at 25 $^{\circ}\text{C}$ and 45 $^{\circ}\text{C}$ in distilled water, respectively. It can be seen that the copolymer forms spherical vesicles with a larger diameter (average: \sim 186.6 nm by DLS) at temperatures below LCST [Figure 11(a)]; when the temperature was increased to a temperature above the LCST (e.g., 45 $^{\circ}\text{C}$), the spherical vesicles became smaller with an average diameter of 137.7 nm as measured by DLS [Figure 11(b)]. This result seems contradictory to the previous observation that the aqueous solution of the block copolymers changes from clear to turbid when the temperature was raised from 25 to 45 $^{\circ}\text{C}$. It is known that that the dark rings or circles of a polymer vesicle formed in aqueous solutions is from the hydrophobic chain in the TEM image, whereas the hydrophilic chains are soluble in water and, therefore, invisible in the TEM image.^{40,41} That means that the diameter of the vesicle's core, formed primarily from the hydrophobic PCL chains, was reduced substantially from 25 to 45 $^{\circ}\text{C}$, reflecting the powerful squeezing effect of the PNIPAM exterior shell on the hydrophobic core. In a sense the PNIPAM chains subsequently become part of the hydrophobic core. However, a particle size reduction does not necessarily mean that a solution would become clear. According to Rayleigh scattering, the light scattering power is proportional to d^6 (d = particle diameter) and to the refractive index difference of the two components. Only when the diameter of particles is smaller than a tenth of the wavelength of the light, scattering will be significantly reduced

and the transparency is thus typically retained in a solution.⁴² That means that the diameter of the self-assembled nanoparticles or vesicles in the current triblock copolymer solutions has to be below 50 nm for the solution to be transparent to visible lights. This rules out the argument that the solution should become much less turbid at 45 $^{\circ}\text{C}$ than at 25 $^{\circ}\text{C}$ since the particle size is much larger than 50 nm (\sim 186.6 nm at 25 $^{\circ}\text{C}$ vs. 137.7 nm at 45 $^{\circ}\text{C}$) and consequently the corresponding light scattering difference between them would be trivial. As a result, the visual appearance change of the block copolymer solutions from clear to turbid when the temperature was raised from 25 to 45 $^{\circ}\text{C}$ is more a solubility effect, and the copolymer becomes more hydrophobic and less soluble in water, leading to turbidity and lower optical transparency (Figures 9 and 10).

Figure 12 shows the size and its size distribution of the self-assembled nanovesicle of mPEO_{3k}-*b*-PCL_{5k}-*b*-PNIPAM_{13.2k} triblock copolymers at temperatures below and above the LCST, measured by DLS. It was found that the nanovesicles are narrowly distributed at both 25 and 40 $^{\circ}\text{C}$. The average size for the nanovesicles is around 138.9 nm at 40 $^{\circ}\text{C}$ (above LCST), which is smaller than the size (\sim 177.7 nm) at 25 $^{\circ}\text{C}$ (below LCST). This result is consistent with the TEM analysis. The detailed measurements of the nanovesicles from the three different triblock copolymers are summarized in Table IV.

Evaluation of the Nanovesicles as a Drug Release Carrier

To evaluate the nanovesicles as a drug release carrier, IMC, a popular anti-inflammation drug, was selected as a model

**Figure 12.** Size distribution of mPEO_{3k}-*b*-PCL_{5k}-*b*-PNIPAM_{13.2k} nanovesicles in distilled water (1 mg/mL) at 25 $^{\circ}\text{C}$ (A) and at 40 $^{\circ}\text{C}$ (B), by DSL.

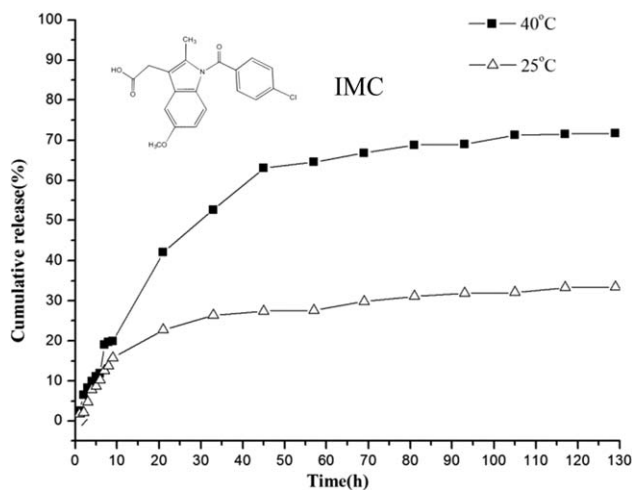


Figure 13. Release of IMC from $mPEO_{3k}$ - b - PCL_{5k} - b - $PNIPAM_{13.2k}$ self-assembled nanovesicles at 40°C (above LCST) and at 25°C (below LCST).

medicine. The physical entrapment of IMC into $mPEO$ - b - PCL - b - $PNIPAM$ nano-vesicles was achieved by a dialysis technique. For this study, only the block copolymer $mPEO_{3k}$ - b - PCL_{5k} - b - $PNIPAM_{13.2k}$, which has a LCSTs close to the physiological temperature, was used. The loading content, which defines as the weight ratio of the loaded amount of IMC to the amount of the block vesicles, is 9.1%. The loading efficiency, which defines as the percent ratio of the loaded amount of IMC to the initial feeding amount of IMC, is 40%, respectively. Figure 13 shows the release profile of IMC with time at temperatures above and below the LCST from the copolymer self-assembled (SA) nanovesicles. A faster release rate of IMC at 40°C (above LCST) than at 25°C (below LCST) was observed, indicating that the nanovesicles has a good response to the thermostimulus.

One would argue that at 40°C, whereby the thermoresponsive PNIPAM chains may collapse onto the PCL surface and create an additional barrier layer for the self-assembled nanovesicles, the release of the hydrophobic drug IMC from the core would be slower. However, the pumping force exerted during the process of PNIPAM chains collapse squeezed the core and subse-

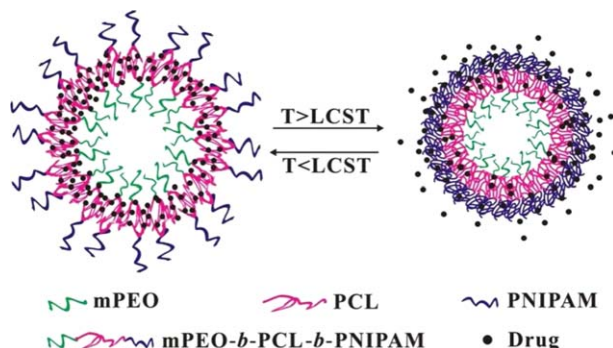


Figure 14. Self-assembly (SA) of the copolymer and the thermally induced drug release of resulting micelles in aqueous solution.

quently accelerates the drug diffusion through the hydrophilic PEO channels. For the current triblock copolymer systems, where the length of PNIPAM block was carefully selected, it appears that the squeezing force induced by the PNIPAM chains collapse surpasses its barrier effort. As a result, release acceleration for the drug release was observed at a temperature above its LCST. Of course if the PNIPAM block is too long, the reverse would be observed.

A scheme illustrating the self-assembly and thermally induced drug release process of the nanovesicles is presented in Figure 14. At a temperature below the LCST, IMC is entrapped within the hydrophobic macromolecular membrane of PCL via hydrogen bonding. When the temperature is raised to above the LCST, the PNIPAM chain becomes hydrophobic from hydrophilic and then collapses onto the PCL membrane. This leads to the shrinkage of the copolymer nanovesicles, and subsequently squeezing out and diffusing the drug into the aqueous system. Furthermore due to the presence of hydrophilic PEO segment in the triblock copolymer, the self-assembled nanovesicles are well dispersed into the solution, and are stable even at higher temperatures, preventing the hydrophobic membrane from forming aggregation or precipitation in the solution. Another point worthy of note is the shell-core membrane structure of the ABC triblock copolymers in aqueous solutions. Since the

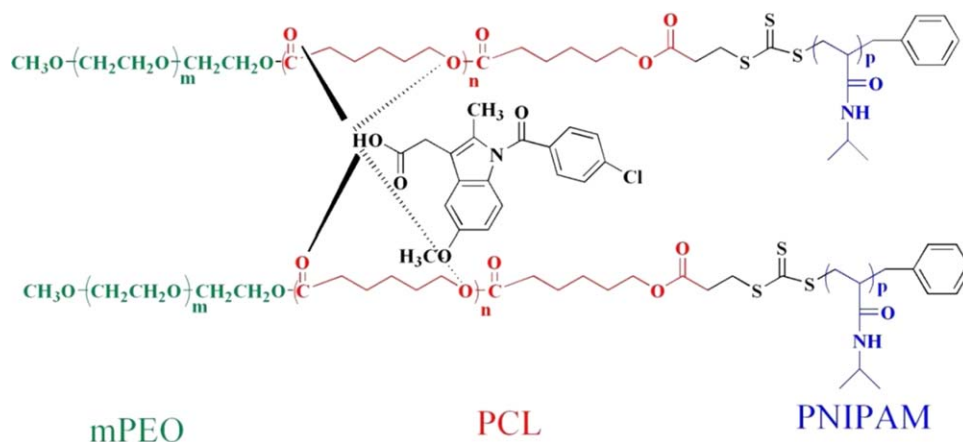


Figure 15. Possible hydrogen bonding between IMC and PCL segments of the triblock copolymers.

mPEO-*b*-PCL-*b*-PNIPAM triblock copolymers were constructed according to the proposed requirements for forming self-assembled asymmetrical vesicles, the PNIPAM block was intentionally built to be longer than the second hydrophilic PEO block so that the self-assembled vesicles of the triblock copolymers in aqueous solutions are most likely to form a structure in which the hydrophobic PCL chains are present as the vesicles core, the PEO chains are in the interior of the vesicles, and PNIPAM chains are in the exterior of the vesicles, if the chain random motion can be neglected.³² This hypothesis was supported by the TEM results, which shows that the PNIPAM chains are presented as the exterior layer of the nanovesicles, which collapse upon heating to form more compact vesicles due to its thermoresponsive behavior. The possible hydrogen bonding between IMC and the PCL segment of the triblock copolymer is presented in Figure 15.

CONCLUSIONS

In summary, a number of novel mPEO-*b*-PCL-*b*-PNIPAM triblock copolymers were synthesized by a combination of ROP and RAFT polymerization techniques. The molecular weight of the triblock copolymers was well controlled by varying the reaction time and conditions. The triblock copolymers undergo self-assembly forming stable nanovesicles of various sizes in aqueous solutions. The nanovesicle has a lipid membrane structure as body cells, and is thermoresponsive, that is, its size is tunable using the temperature as a switch: shrinks at a temperature above the LCST and expands at a temperature below the LCST. It is demonstrated with IMC that the nanovesicles can potentially be used as an effective and intelligent drug release carrier.

ACKNOWLEDGMENTS

The financial support for this work, provided by the Henan Science Foundation of the People's Republic of China for Outstanding Youth (74100510025) and the Natural Science Foundation of Education Department of Henan Province (2009A430018), is highly appreciated. The authors thank Guanyu Yang for variable temperature UV measurements, Yanxia Cao for TEM analysis, and Peng Fu for GPC analysis.

REFERENCES

1. Sun, P.; Zhang, Y.; Shi, L.; Gan, Z. *Macromol. Biosci.* **2010**, *10*, 621.
2. Sundararaman, A.; Stephan, T.; Grubbs, R. B. *J. Am. Chem. Soc.* **2008**, *130*, 12264.
3. Chang, C.; Wei, H.; Quan, C.; Li, Y.; Liu, J.; Wang, Z.; Cheng, S.; Zhang, X.; Zhuo, R. *J. Polym. Sci. Part A: Polym. Chem.* **2008**, *46*, 3048.
4. Onaca, O.; Enea, R.; Hughes, D. W.; Meier, W. *Macromol. Biosci.* **2009**, *9*, 129.
5. Liu, J.; Lee, H.; Allen, C. *Curr. Pharm. Des.* **2006**, *12*, 4685.
6. Sun, T.; Guo, Q.; Zhang, C.; Hao, J.; Xing, P.; Su, J.; Li, S.; Hao, A.; Liu, G. *Langmuir* **2012**, *28*, 8625.
7. Liu, G.; Jin, Q.; Liu, X.; Li, L.; Chen, C.; Ji, J. *Soft Matter* **2011**, *7*, 662.
8. He, C.; Zhuang, X.; Tang, Z.; Tian, H.; Chen, X. *Adv. Healthcare Mater.* **2012**, *1*, 48.
9. Gary, D. J.; Lee, H.; Sharma, R.; Lee, J.-S.; Kim, Y.; Cui, Z. Y.; Jia, D.; Bowman, V. D.; Chipman, P. R.; Wan, L.; Zou, Y.; Mao, G.; Park, K.; Herbert, B.-S.; Konieczny, S. E.; Won, Y.-Y. *ACS Nano* **2011**, *5*, 3493.
10. Otsuka, H.; Nagasaki, Y.; Kataoka, K. *Adv. Drug Deliv. Rev.* **2003**, *55*, 403.
11. Soo, P. L.; Eisenberg, A. *J. Polym. Sci. Part B: Polym. Phys.* **2004**, *42*, 923.
12. Discher, D. E.; Eisenberg, A. *Science* **2002**, *297*, 967.
13. Tanner, P.; Baumann, P.; Enea, R.; Onaca, O.; Palivan, C.; Meier, W. *Acc. Chem. Res.* **2011**, *44*, 1039.
14. Kumar, M.; Grzelakowski, M.; Zilles, J.; Clark, M.; Meier, W. *Proc. Nat. Acad. Sci. USA* **2007**, *104*, 20719.
15. Ahmed, F.; Discher, D. D. *J. Controlled Release* **2004**, *96*, 37.
16. Cho, H. K.; Lone, S.; Kim, D. D.; Choi, J. H.; Choi, S. W.; Cho, H. H.; Kim, J. H.; Cheong, I. W. *Polymer* **2009**, *50*, 2357.
17. Mansour, H. M.; Sohn, M. J.; Al-Ghananeem, A.; DeLuca, P. *Int. J. Mol. Sci.* **2010**, *11*, 3298.
18. Xu, Y.; Dong, C. *J. Polym. Sci. Part A: Polym. Chem.* **2012**, *50*, 1216.
19. Rohner, D.; Hutmacher, D. W.; Cheng, T. K.; Oberholzer, M.; Hammer, B. *J. Biomed. Mater. Res. Part B: Appl. Biomater.* **2003**, *66B*, 574.
20. Leroux, J.-C.; Roux, E.; Garrec, D. L.; Hong, K.; Drummond, D. C. *J. Controlled Release* **2001**, *72*, 71.
21. Lu, Y.; Ou, T.; Tan, J.; Hou, J.; Shao, W.; Peng, D.; Sun, N.; Wang, X.; Wu, W.; Bu, X.; Huang, Z.; Ma, D.; Wong, K.; Gu, L. *J. Med. Chem.* **2008**, *51*, 6381.
22. Thomas, V.; Dean, D. R.; Vohra, Y. K. *Curr. Nanosci.* **2006**, *2*, 155.
23. Zhang, X.; Zhuo, R. *Langmuir* **2001**, *17*, 12.
24. Qin, S.; Geng, Y.; Discher, D. E.; Yang, S. *Adv. Mater.* **2006**, *18*, 2905.
25. Topp, M.; Dijkstra, P.; Talsm, H.; Feijen, J. *Macromolecules* **1997**, *30*, 8518.
26. Virtanen, J.; Holappa, S.; Lemmetyinen, H. *Macromolecules* **2002**, *35*, 4763.
27. Zhang, W.; Shi, L.; Wu, K.; An, Y. *Macromolecules* **2005**, *38*, 5743.
28. Zheng, Q.; Zheng, S. *J. Polym. Sci. Part A: Polym. Chem.* **2012**, *50*, 17.
29. Zhang, Y.; Jiang, M.; Zhao, J.; Ren, X.; Chen, D.; Zhang, G. *Adv. Funct. Mater.* **2005**, *15*, 695.
30. Teodorescu, M.; Negru, I.; Stanescu, P.; Draghici, C.; Anamaria Lungu, A.; Sarbu, A. *React. Funct. Polym.* **2010**, *70*, 70790.
31. Goertz, M. P.; Marks, L. E.; Montano, G. A. *ACS Nano* **2012**, *6*, 1532.

32. Stoenescu, R.; Graff, A.; Meier, W. *Macromol. Biosci.* **2004**, *4*, 930.
33. Stoenescu, R.; Meier, W. *Chem. Commun.* **2002**, *24*, 3016.
34. Liu, F.; Eisenberg, A. *J. Am. Chem. Soc.* **2003**, *125*, 15059.
35. Wittmann, A.; Azzam, T.; Eisenberg, A. *Langmuir* **2007**, *23*, 2224.
36. Lai, J. T.; Filla, D.; Shea, R. *Macromolecules* **2002**, *35*, 6754.
37. Chiefari, J.; Chong, Y. K.; Ercole, F.; Krstina, J.; Jeffery J.; Le, T. P. T.; Mayadunne, E. T. A.; Meijs, G. F.; Moad, C. L.; Moad, G.; Rizzardo, E.; Thang, S. H. *Macromolecules* **1998**, *31*, 5559.
38. Zhang, Y.; Sun, P.; Gan, Z. *Sci. China Chem.*, **2010**, *53*, 519.
39. Schild, H. G.; Tirrell, D. A. *J. Phys. Chem.* **1990**, *94*, 4352.
40. Du, J. Z.; Chen, Y. M.; Zhang, Y. H.; Han, C. C.; Fischer, K.; Schmidt, M. *J. Am. Chem. Soc.* **2003**, *125*, 14710.
41. Du, J. Z.; O'Reilly, R. K. *Soft Matter* **2009**, *5*, 3544.
42. Kumar, P.; Mittal, K. L. *Handbook of Microemulsion Science and Technology*; Marcel Dekker: New York, **1999**.